Imaging characteristics of cerebral autosomal dominant arteriopathy with subcortical infarcts and leucoencephalopathy (CADASIL)

Dragan Stojanov[1,2,*], Aleksandra Aracki-Trenkic[2], Slobodan Vojinovic[1,3], Srdjan Ljubisavljevic[1,3], Daniela Benedeto-Stojanov[1], Aleksandar Tasic[2], Sasa Vujnovic[4]

[1]Faculty of Medicine, University of Niš, Niš, Serbia, [2]Center of Radiology, Clinical Center, Niš, Serbia, [3]Clinic of Neurology, Clinical Center, Niš, Serbia, [4]Institute of Clinical Radiology, University Clinical Center Banja Luka, Banja Luka, Bosnia and Herzegovina

ABSTRACT

Cerebral autosomal dominant arteriopathy with subcortical infarcts and leucoencephalopathy (CADASIL) is an autosomal dominant vascular disorder. Diagnosis and follow-up in patients with CADASIL are based mainly on magnetic resonance imaging (MRI). MRI shows white matter hyperintensities (WMHs), lacunar infarcts and cerebral microbleeds (CMBs). WMHs lesions tend to be symmetrical and bilateral, distributed in the periventricular and deep white matter. The anterior temporal lobe and external capsules are predilection sites for WMHs, with higher specificity and sensitivity of anterior temporal lobe involvement compared to an external capsule involvement. Lacunar infarcts are presented by an imaging signal that has intensity of cerebrospinal fluid in all MRI sequences. They are localized within the semioval center, thalamus, basal ganglia and pons. CMBs are depicted as focal areas of signal loss on T2 images which increases in size on the T2*-weighted gradient echo planar images ("blooming effect").

INTRODUCTION

Cerebral autosomal dominant arteriopathy with subcortical infarcts and leucoencephalopathy (CADASIL) is a hereditary vascular disorder, inherited as an autosomal dominant trait, clinically characterized by a number of following symptoms: migraine with aura, mood disorder, vascular dementia, ischemic stroke and premature death [1-4]. The second most frequent manifestation of CADASIL is cognitive impairment with executive dysfunction and slowness of cognitive processing speed present in most patients [5]. The precise prevalence of CADASIL is not ascertained. Cases of CADASIL have been reported in a wide variety of ethnic groups throughout the world [6]. One study showed the estimated prevalence of CADASIL in Scotland is approximately 1.98 per 100,000 adults, with the prevalence of a probable mutation being 4.14 per 100,000 adults [7]. However, this estimation cannot be generalized worldwide. Before the establishment of genetic testing for CADASIL in 2000, many cases of were misinterpreted as multiple sclerosis, Alzheimer's disease, or other neurodegenerative diseases.

CADASIL is the most frequent single-gene disorder of small cerebral arteries. It develops due to mutations within the epidermal growth factor-like repeat domain of the *NOTCH3* gene located on chromosome 19p13 [8]. *NOTCH3* gene encodes a large single-pass transmembrane receptor of 2,321 amino acids. There are four members of the NOTCH receptor family in mammals (NOTCH 1-4). This particular gene consists of a transmembrane domain, an intracellular domain and a large extracellular domain (ECD) composed of 34 tandem epidermal growth factor (EGF)-like repeats and three Notch/Lin12 repeats. The length of an each EGF repeat is approximately 40 amino acids. There are six cysteine residues, forming three sulphur bridges in a highly organized way in each of the repeats. Ligand binding causes a proteolytic cleavage which leads to the translocation of the intracellular domain to the nucleus. A significant reduction

*Corresponding author: Dragan Stojanov, Center of Radiology, Clinical Center Niš, Bul. Dr. Z. Đinđića 48, 18000 Nis, Serbia.
Tel. +381631094197
E-mail: drstojanov@gmail.com

in transcriptional activity is produced by a small number of mutations occurring in the ligand-binding domain (EGF repeats 10 and 11) [9-11] (Figure 1).

Normal maturation of brain arteries depends heavily on NOTCH3 gene in both fetal and adult mammals. There is a broad spectrum of CADASIL mutations. More than 150 different mutations in 18 exons have been already described [12,13,14]. Exon 4 is the most frequently affected location of *NOTCH3* gene mutation in European population, followed by exons 8 and 3 [15]. De novo mutations of the *NOTCH3* gene are very rare [16-18].

Morphologically, the vascular lesion causing CADASIL is a non-arteriosclerotic, non-amyloid arteriopathy. Small perforating cerebral arteries are most frequently affected, with an accumulation of granular and osmiophilic substances within the vascular smooth muscle cell membrane (VSMC) as the basic pathological finding [19,20]. This initial fattening and expansion of the extracellular matrix might be present to a lesser degree in extracerebral arteries such as skin arterioles [21]. VSMC gradually undergo degeneration with mural fibrosis. It results in stenosis of the distal segment of medullary arteries. Cerebral vessels lose ability of autoregulaton

becoming thus functionally blood pressure-dependent [13]. These small vessels changes lead to small infarcts in the white matter, deep gray matter and the pons.

DIAGNOSIS OF CADASIL

The diagnosis of CADASIL is made on the basis of a typical clinical picture and the features of a magnetic resonance imaging (MRI) of the brain and is confirmed by the biopsy (of the sural nerve, muscles and skin) as well as by a genetic analysis (Figure 2).

The clinical diagnosis of CADASIL is based on the following conditions: (1) clinical onset at a specific age (40-50 years); (2) absence of stroke risk factors; (3) frequent lacunar infarction episodes gradually leading to pseudobulbar paralysis and dementia (migraine, emotional disturbance, cerebral infarction, and dementia in 30%, 20%, 85%, and 30-90% of patients, respectively); and (4) familial distribution of the disease or similar symptoms (autosomal dominant inheritance) [21].

Imaging and laboratory examinations play an essential role in diagnosis of CADASIL: the key diagnostic features include
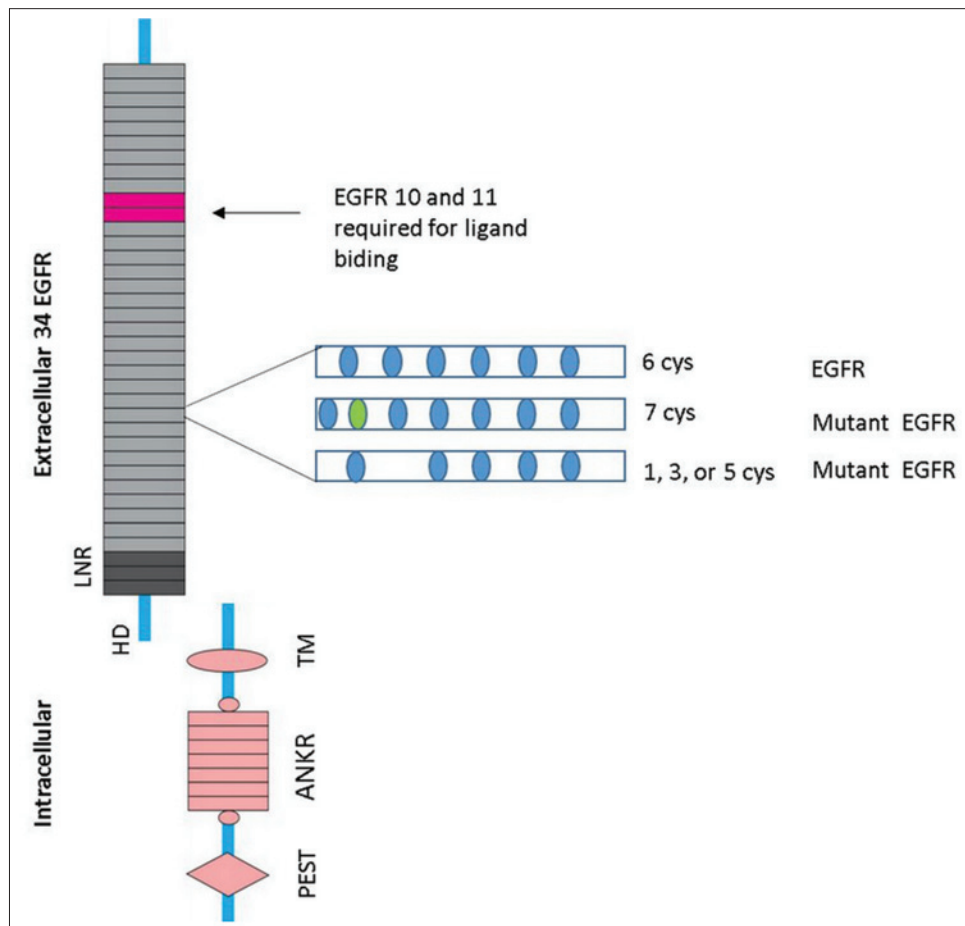

FIGURE 1. The NOTCH3 receptor and CADASIL mutation EGFR-epidermal growth factorlike repeat, LNR- Lin12 repeats, HD-heterodimerisation domain, TM-transmembrane domain, ANKR-ankyrin repeats, PEST-sequence that is rich in proline, glutamic acid, serine, and threonine.
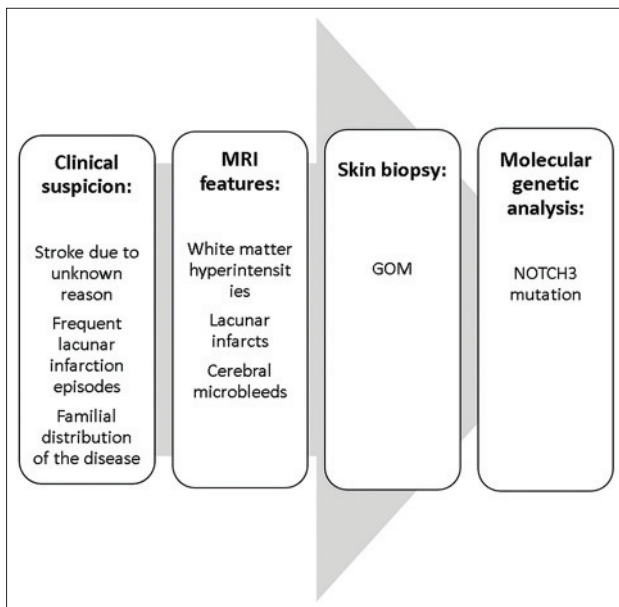
FIGURE 2. Algorithm of CADASIL diagnosis

(1) Leukoaraiosis and multiple small infarcts presented bilaterally in deep white matter, basal ganglia, thalamus, and pons on MRI; (2) granular and osmiophilic substance layers around the vascular smooth muscles in the brain, skeletal muscle, peripheral nerves, and skin verified by electron microscopy; and (3) *NOTCH3* mutations confirmed by DNA analysis [22].

Since the cutaneous surface sampling is much easier than the central nervous system's tissue sampling, a skin biopsy is a significant method facilitating the diagnosis [23].

Diagnostic gold standard of the disease remains the genetic analysis, but it is expensive and may be false negative if only a cluster of most probably affected exons is examined [22].

IMAGING CHARACTERISTICS OF CADASIL

Reaching the diagnosis and follow-up in patients with CADASIL relies mainly on MRI findings [24,25]. Sensitivity and specificity are higher than in computerized tomography (CT).

Neuroimaging shows three types of lesions in patients with CADASIL. The first type is white matter hyperintensities (WMHs) on MRI (Figure 3 and Figure 4) and white-matter hypodensities on CT (Figure 5a, 5b and 5c). The second type of lesions is lacunar infarcts in the semioval center, thalamus, basal ganglia, and pons, while the third type is represented with cerebral microbleeds (CMBs). The presence of WMHs may be associated with lacunar infarction while CMBs may be present in both symptomatic and asymptomatic patients with a confirmed *NOTCH1* mutation [26-28].

WHITE MATTER HYPERINTENSITIES

WMHs are one of the first imaging signs of CADASIL, often appearing before its clinical onset. Presented as white-matter regions of higher signal intensities on T2W and FLAIR sequences, these lesions tend to be symmetrical and bilateral. WMHs are found usually in the periventricular region (Figure 3b, 3d, 3g, 3f) and in deep white matter (Figure 3c, 3e, 3h), but less frequently in superficial white matter [29-32]. Predominantly affected regions are frontal, parietal, and anterior temporal, followed by external capsule. Recognition of these lesions in younger patients is of great importance for early diagnosis of CADASIL. The occipital lobe is markedly less severely affected.

However, there is a relative sparing of the arcuate fibers and cortex [33]. Cortical sparing is particularly striking when viewed in coronal and sagittal section. Cortical lesions are extremely rare in CADASIL, even in those patients with most extensive abnormalities [34]. That could be explained by the anatomically different cortical and subcortical blood supply. Clear cortical and subcortical arterial territories can be differentiated, the latter being supplied by the short and long corticomedullary branches.

It has been observed that patients with CADASIL have larger WM volume. WM volume may increase due to intramyelinic edema in the white matter detected early in the course of the disease [35].

Recent studies have recognized the anterior temporal lobe (Figure 3a and Figure 5a) and external capsules (Figure 4b, Figure 4c and Figure 5b) as sites of predilection for WMHs [30,36], which, if affected, are very useful in differentiation from other forms of small-vessel disease [36,37]. According to Marcus et al., anterior temporal lobe involvement has a much higher specificity than external capsule involvement [38], specificity being 100% in contrast to 45% respectively, while sensitivity is approximately the same (90% opposed to 93%) [33]. Anterior temporal lobe involvement may occasionally be absent, especially in the Asian CADASIL population [24]. The diagnosis of CADASIL should be taken into account in patients with lacunar infarcts, leukoencephalopathy and migraine with an atypical aura even in the absence of white matter lesions in the anterior temporal poles [39]. Findings of Yamamoto M et al. [19] suggest that temporal lobe WMHs relate to the numerous fluid-filled perivascular spaces (PVS) or increased number of PVS rather than the presence of lacunar infarcts. On MRI, PVS may be seen as T1W hypointense and T2W hyperintense areas, similar to small infarcts or lacunes. Enlarged PVS are evident in temporal pole because of its unique convolutional structure and vascularization by the branches of the anterior temporal artery. Increased PVS may reflect WMHs on MRI [37] since
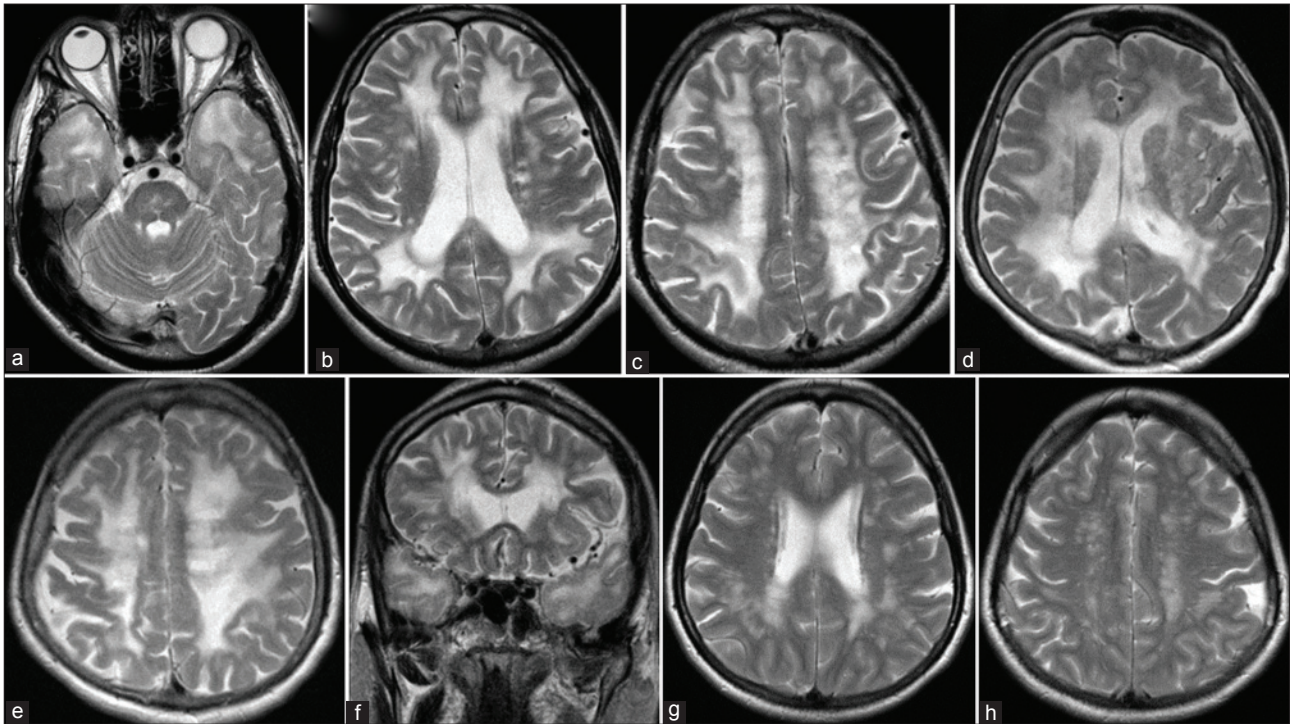
FIGURE 3. MRI of three different patiens from one family (mother, son, doughter). a) axial T2-weighted image shows characteristic changes in CADASIL - anterior temporal pole hyperintensities; b,d,g) axial T2-weighted images show periventricular hyperintensities; f) coronal T2-weighted image shows periventricular hyperintensities; c,e,h) axial T2-weighted images show hyperintensities in the deep white matter.

the resolution of MRI is currently not sufficiently high [40] to distinguish single large fluid-filled space (~2 mm) from cluster small spaces. Subcortical lacunar lesions in the temporal lobes are best visualized by a technique of hydrographic 3D high-resolution turbo spin echo (TSE) with variable flip angle sequence (SPACE) [41].

Other regions such as the posterior temporal and occipital white matter, the basal ganglia nuclei, the thalamus and internal capsule, as well as the pons, show only moderate involvement. However, corpus callosum and infratentorial areas are less frequently affected in CADASIL. Callosal commissure involvement is of particular diagnostic importance [25]. It is seen as hyperintense lesions on T2W imaging and hypointense lesions on T1W imaging involving the full thickness of the corpus callosum. The involvement of corpus callosum is a characteristic feature of multiple sclerosis - the lesions classically involve the undersurface of this structure. Lesions of corpus callosum are rarely seen in a narrow variety of small vessel diseases. Short penetrating arterioles of <100 μm in diameter, supplying the central corpus callosum, have good anastomotic connections and are not prone to atherosclerotic disease [42]. In addition, thrombosis in situ of the branches of the anterior cerebral artery, which supply the greater part of corpus callosum, is very unusual. Underlying pathology in CADASIL is a concentric deposition of granular material within the media of small to medium arterioles leading to stenosis.

Confluent areas of WMHs that are seen on T2W imaging correspond to hypointense areas on T1W imaging (Figure 4a). Lesions are less extensive on T1W than T2W imaging. A significant loss of contrast between gray matter and normal-appearing white matter was seen on 3D T1 imaging. This is very likely due to the tissue changes in normal-appearing white matter outside signal abnormalities on T2 or FLAIR sequences. [43].

In patients with CADASIL, the dilation of perivascular spaces (dPVS) throughout the brain, varying in its extent according to the cerebral location, may be promoted by the progression of the hereditary microangiopathy with aging. One of the common MRI features found in temporal lobes and subinsular areas are dPVS, which may share a similar pathogenesis with the extension of WMH during the course of the disease. In this model of small-vessel disease, there is a possibility of dPVS participation in the cognitive decline development. Moreover, the large number of dPVS in white matter signals a higher risk of cognitive decline in CADASIL [44].

LACUNAR INFARCTS

Lacunar infarcts are parenchymal defects that do not reach the cortical gray matter, presented by an imaging signal of cerebrospinal fluid intensity in all MRI sequences, with a diameter of more than 2 mm [8]. Lacunar infarcts
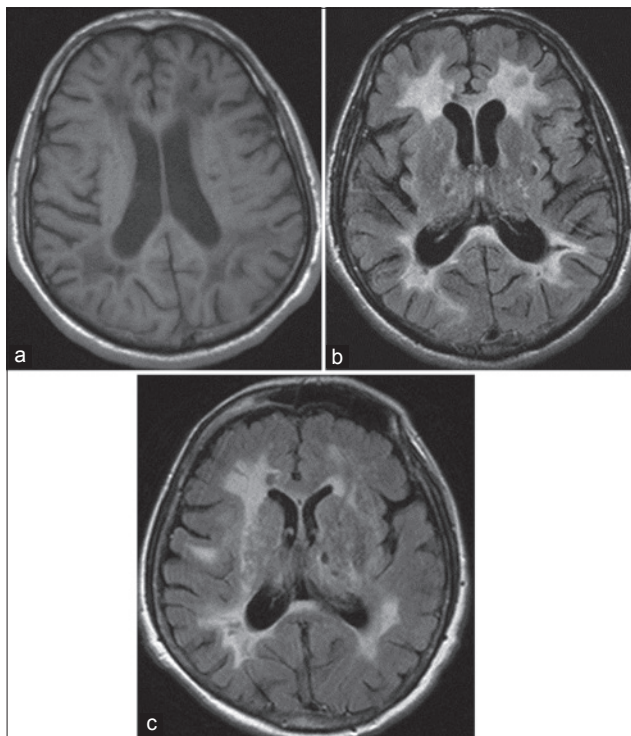
FIGURE 4. a) Axial T1-weighted image shows periventricular hypointensities; b,c) axial FLAIR images show periventricular hyperintensities and characteristic hyperintensities of the external capsule; c) axial FLAIR image shows lacunar infarcts in basal ganglia.
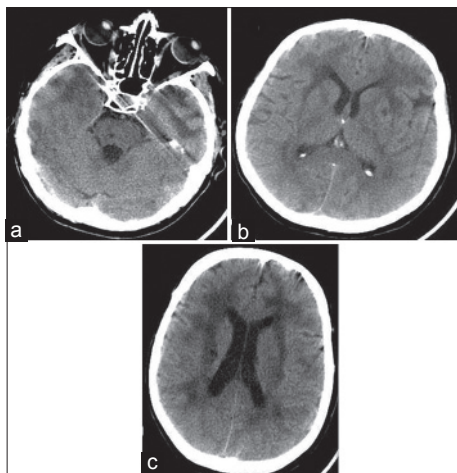

FIGURE 5. Axial non-contrast CT images show a) temporal pole hyperintensities and lacunar infarction in pons; b) periventricular hyperintensities with involvement of the external capsule; c) hyperintensities in the white matter, and lacunar infarcts in basal ganglia.

in CADASIL are localized within the semioval center, thalamus, basal ganglia and pons (Figure 4c, Figure 5a and Figure 5b) [33]. Areas smaller than 2 mm in diameter, present in the lower third of corpus striatum of the basal ganglia and demonstrating isointensity to cerebrospinal fluid, differentiate normally dilated Virchow–Robin spaces from lacunar infarcts [45]. The number of lacunar infarction on MRI in patients with CADASIL is more important predictor of cognitive impairment [24].

CEREBRAL MICROBLEEDS (CMBS)

Gradient echo planar T_2^* MRI enables the detection of tiny foci of blood within the brain, which have been termed cerebral microbleeds. CMBs are found in 31-69% of patients with CADASIL. They are depicted as focal areas of signal loss on T_2 imaging, increasing in size in T_2^*- weighted gradient echo planar images ("blooming effect"), with a diameter smaller than 10 mm [46]. This way CBMs differ from regions of signal loss originating from vascular flow void. CBMs may be located in various portions of the brain. Cortical/subcortical areas, white matter, thalamus, and brainstem are preferential sites [47,48]. Typically, they are always found outside the ischemic lesions [28].

According to recently published research, cortex alterations may be related to early symptoms of the disease. These data, obtained by seven Tesla MRI, show diffuse T_2^* alterations within the cortical mantle. However, the origin of these alterations is still not determined [49]. Rarely, spontaneous intracerebral hemorrhage (ICH) can occur in patients with CADASIL. Therefore, for the prediction of the risk of ICH, MRI screening for CMBs can be helpful [50, 51].

The detection of petechial intraparenchymal hemorrhages is a diagnostically and prognostically useful marker, since the identification of microvascular pathology in an asymptomatic or minimally symptomatic stage of the disease enables a window of therapeutic opportunity to be created [52].

ADVANCED MR TECHNIQUES

There are advanced MR techniques able to detect in vivo macroscopic damage that remains unnoticed using conventional radiological techniques. Relevant parameters for the assessment of cerebral small vessel diseases (cSVD) can be provided by ADC histograms from daily used DWI [53]. Diffusion tensor imaging (DTI), magnetization transfer imaging (MTI) and magnetic resonance spectroscopy (MRS) have shown that microstructural changes are present in both normal and abnormal white matter, probably reflecting neuronal loss and demyelination. The degree of the underlying ultrastructural alterations is related to the clinical severity. Ultrastructural tissue damage may be demonstrated using DTI, even in regions appearing normal in conventional MRI [28]. Holtmannspotter at al. [54] reported that DTI histogrammetrics predict disease progression in CADASIL.

The study of Liem MK et al. has demonstrated increased iron accumulation in the putamen and caudate nucleus in patients with the small vessel disease, which is in accordance with the previous hypothesis on the increased iron accumulation in the pathogenesis of small vessel disease [55].

One of the novel and very useful MRI techniques is

TABLE 1. Radiology features of CADASIL and its diagnostic mimickers

MRI features	CADASIL	Mimickers				
		MS	Vascular disease	MELAS	Fabry disease	Internal watershed ischemia
WMHs	Anterior temporal lobe external capsule	Corpus callosum U-fibers spinal cord brainstem cerebellum	Deep grey matter semioval center corona radiata callosal commissure	Cortical subcortical	Subcortical periventricular	Deep unilateral
Lacunar infarcts	Semioval center thalamus basal ganglia pons					
CMBs	Outside of ischemic lesion					

MRI - Magnetic resonance imaging, CADASIL - Cerebral autosomal dominant arteriopathy with subcortical infarcts and leukoencephalopathy, MS - Multiple sclerosis, MELAS - Mitochondrial encephalomyelopathy with lactic acidosis and stroke like episodes, WMHs - White matter hyperintensities, CMBs - Cerebral microbleeds

q-Space imaging. The purpose of this technique is to assess the ultrastructural changes of the white matter. So far, q-Space imaging has proved to be a method sensitive to an early neuronal damage in a characteristic distribution. Therefore, the method can be used as a significant assistance in monitoring of the patients in the preclinical stage as well as in the assessment of the effects of possible future medical interventions [56].

DIFFERENTIAL DIAGNOSIS

The list of differential diagnosis of T2W confluent white matter hyperintensities is large, comprising other causes of vascular involvement and inflammatory diseases. The major differential diagnosis includes demyelinating and vascular diseases. Multiple sclerosis (MS) has a typical distribution of white matter hyperintensities – corpus callosum, U-fibers, temporal lobes, brainstem, cerebellum and spinal cord. Periventricular lesions in MS are ovoid and perpendicular to ventricles. Active lesions demonstrate post-contrast enhancement.

In vascular diseases, focal white matter hyperintensities are identified in the deep gray matter structures, corona radiata, and semioval center. Anterior temporal pole involvement is rare in sporadic small vessel disease. The presence of callosal commissure lesions is differentiating CADASIL from small-vessel disease [25].

Other rare causes of white matter hyperintensities include cerebral vasculitis, primary angiitis, leucodystrophies, infective conditions such as Lyme disease and the neurosarcoidosis. Fabry disease and mitochondrial encephalomyelopathy with lactic acidosis and stroke-like episodes (MELAS) are rare genetical causes. Multifocal cortical and subcortical T2 hyperintensities are seen in MELAS. Swollen gyri in the acute phase, cortical laminar necrosis with cortical T1W hyperintensities in the subacute phase, cortical atrophy in the chronic phase are identified in MELAS. Familial hemiplegic migraine (FHM) is another clinical diagnosis to be considered in the differential. However, FHM is usually inherited and does not progress to dementia and pseudo-bulbar palsy. Multifocal

subcortical and periventricular white matter hyperintensities are identified in FHM with no associated diffusion signal changes or enhancement. Internal watershed ischemia caused by carotid disease should also be considered in the differential diagnosis - it can result in deep white matter hyperintensity, but it is usually unilateral (Table 1).

CONCLUSION

Diagnosis and follow-up in patients with CADASIL are based mainly on MRI findings. Neuroimaging shows WMHs, lacunar infarcts, and CMBs. WMHs lesions tend to be symmetrical and bilateral, distributed in periventricular and deep white matter. The anterior temporal lobe and external capsules are sites of predilection for WMHs, with higher specificity of anterior temporal lobe involvement. Lacunar infarcts in CADASIL are localized within the semioval center, thalamus, basal ganglia, and pons. The number of lacunar infarcts is an important predictor of cognitive impairment in patients with CADASIL.

DECLARATION OF INTERESTS

The authors declare no conflict of interests.

REFERENCES

[1] Desmond DW, Moroney JT, Lynch T, Chan S, Chin SS, Mohr JP. The natural history of CADASIL: a pooled Analysis of previously published cases. Stroke 1999;30(6):1230-1233. http://dx.doi.org/10.1161/01.STR.30.6.1230.

[2] Opherk C, Peters N, Herzog J, Luedtke R, Dichgans M. Long term prognosis and causes of death in CADASIL: a retrospective study in 411 patients. Brain 2004;127(11):2533-2539. http://dx.doi.org/10.1093/brain/awh282.

[3] Kalaria RN, Viitanen M, Kanlimo H, Dichagens M, Tabira T. The pathogenesis of CADASIL: an update. J Neurol Sci 2004;226(1-2):35-39. http://dx.doi.org/10.1016/j.jns.2004.09.008.

[4] Chabriat H. Cerebral autosomal dominant arteriopathy with subcortical infarcts and leukoencephalopathy. Geriatr Psychol Neuropsychiatr Vieil 2014;12(2):183-192.

[5] Peters N, Opherk C, Danek A, Ballard C, Herzog J, Dichgans M. The pattern of cognitive performance in CADASIL: a monogenic condition leading to subcortical ischemic vascular dementia. Am

J Psychiatry 2005;162(11):2078-2085. http://dx.doi.org/10.1176/appi.ajp.162.11.2078.

[6] Kim YE, Yoon CW, Seo SW, Ki CS, Kim YB, Kim JW, et al. Spectrum of NOTCH3 mutations in Korean patients with clinically suspicious cerebral autosomal dominant arteriopathy with subcortical infarcts and leukoencephalopathy. Neurobiol Aging 2014;35(3):726.e1-6.

[7] Razvi SS, Davidson R, Bone I, Muir KW. The prevalence of cerebral autosomal-dominant arteriopathy with subcortical infarcts and leucoencephalopathy (CADASIL) in the west of Scotland. J Neurol Neurosurg Psychiatry 2005;76(5):739-741. http://dx.doi.org/10.1136/jnnp.2004.051847.

[8] Joutel A, Corperchot C, Ducros A, Vahedi K, Chabriat H, Mouton P, et al. Notch3 mutation in CADASIL, a hereditary adult-onset condition causing stroke and dementia. Nature 1996;383(6602):707-710. http://dx.doi.org/10.1038/383707a0.

[9] Bianchi S, Zicari E, Carluccio A, Di Donato I, Pescini F, Nannucci S, et al. CADASIL in central Italy: a retrospective clinical and genetic study in 229 patients. J Neurol 2015;262(1):134-141. http://dx.doi.org/10.1007/s00415-014-7533-2.

[10] Rutten JW, Haan J, Terwindt GM, van Duinen SG, Boon EM, Lesnik Oberstein SA. Interpretation of NOTCH3 mutations in the diagnosis of CADASIL. Expert Rev Mol Diagn 2014;14(5):593-603. http://dx.doi.org/10.1586/14737159.2014.922880.

[11] Zea-Sevilla MA, Bermejo-Velasco P, Serrano-Heranz R, Calero M. Cerebral Autosomal Dominant Arteriopathy with Subcortical Infarcts and Leukoencephalopathy (CADASIL) associated with a Novel C82R Mutation in the NOTCH3 Gene. J Alzheimers Dis 2015;43(2):363-367.

[12] Herve D, Chabriat H. CADASIL. J Geriatr psychiatry Neurol 2010;23(4):269-276. http://dx.doi.org/10.1177/0891988710383570

[13] Lee YC, Liu CS, Chang MS, Lin KP, Fuh JL, Lu YC, et al. Population-specific spectrum of NOTCH3 mutations, MRI features and founder effect of CADASIL in Chinese. J Neurol 2009;256(2):249-255. http://dx.doi.org/10.1007/s00415-009-0091-3.

[14] Mignarri A, Martini G, Malandrini A, Bellini M, Bianchi S, Tassi R, et al. First report of Iraqi Kurdish CADASIL patient. NeurolSci 2011;32(2):359-360. http://dx.doi.org/10.1007/s10072-010-0399-x

[15] Federico A, Bianchi S, Dotti MT. The spectrum of mutations for CADASIL diagnosis. Neurol Sci 2005;26(2):117-124. http://dx.doi.org/10.1007/s10072-005-0444-3.

[16] Stojanov D, Grozdanovic D, Petrovic S, Benedeto-Stojanov D, Stefanovic I, Stojanovic N, et al. De novo mutation in the NOTCH3 gene causing CADASIL. Bosn J Basic Med Sci 2014;14(1):48-50.

[17] Joutel A, Dodick DD, Parisi JE, Cecillon M, Tournier-Lasserve E, Bousser MG. De novo mutation in the Notch3 gene causing CADASIL. Ann Neurol 2000;47(3):388-391. http://dx.doi.org/10.1002/1531-8249(200003)47:3<388:AID-ANA19>3.0.CO;2-Q.

[18] Coto E, Menéndez M, Navarro R, Garcia-Castro M, Alvarez V. A new de novo Notch3 mutation causing CADASIL. Eur J Neurol 2006;13(6):628-631. http://dx.doi.org/10.1111/j.1468-1331.2006.01337.x.

[19] Yamamoto Y, Ihara M, Tham C, Low RW, Slade JY, Moss T, et al. Neuropathological correlates of temporal white matter hyperintensities in CADASIL. Stroke 2009;40(6):2004-2011. http://dx.doi.org/10.1161/STROKEAHA.108.528299.

[20] Yamamoto Y, Craggs LJ, Watanabe A, Booth T, Attems J, Low RW. Brain microvascular accumulation and distribution of the NOTCH3 ectodomain and granular osmiophilic material in CADASIL. J Neuropathol Exp Neurol 2013;72(5):416-431. http://dx.doi.org/10.1097/NEN.0b013e31829020b5.

[21] Uchino M. The pathomechanism and treatment of CADASIL. Rinsho Shinkeiqaku 2011;51(11):945-948. http://dx.doi.org/10.5692/clinicalneurol.51.945.

[22] Peisker T, Musli L, Hrebicek M, Vlaskova H, Cihelkova I, Bartos A. Clinical spectrum in CADASIL family with a new mutation. Biomed Pup Med Fac Univ Palacky Olomouc Czech Rep 2013;157(4):379-382. doi: 10.5507/bp.2013.055. http://dx.doi.org/10.5507/bp.2013.055.

[23] Choudhary S, McLeod M, Torchia D, Romanelli P. Cerebral Autosomal Dominant Arteriopathy with Subcortical Infarcts and Leukoencephalopathy (CADASIL). J Clin Aesthet Dermatol 2013;6(3):29-33.

[24] Lee JS, Choi JC, Kang SY, Kang JH, Na HR, Park JK. Effects of lacunar infarctions on cognitive impairment in patients with cerebral autosomal-dominant arteriopathy with subcortical infarcts and leucoencephalopathy. J Clin Neurol 2011;7(4):210-214. http://dx.doi.org/10.3988/jcn.2011.7.4.210.

[25] Singhal S, Rich R, Markus HS. The spatial distribution of MR image abnormalities in cerebral autosomal-dominant arteriopathy with subcortical infarcts and leucoencephalopathy and their relationship to age and clinical features. Am J Neuroradiol 2005;26(10):2481-2487.

[26] vanden Boom R, Lesnik Oberstein SA, Ferrari MD, Haan J, van Buchem MA.Cerebral autosomal-dominant arteriopathy with subcortical infarcts and leucoencephalopathy: MRI imaging findings at different ages – 3rd-6th decades. Radiology 2003;229(3):683-690. http://dx.doi.org/10.1148/radiol.2293021354.

[27] Lesnik Oberstein SA, van den Boom R, van Buchem MA,van Houwelingen HC, Bakker E, Vollebregt E, et al.Cerebral microbleeds in CADASIL. Neurology 2001;57(6):1066-1070. http://dx.doi.org/10.1212/WNL.57.6.1066.

[28] Choi JC. Cerebral autosomal dominant arteriopathy with subcortical infarcts and leucoencephalopathy: a genetic cause of cerebral small vesels disease. J Clin Neurol 2010;6(1):1-9. http://dx.doi.org/10.3988/jcn.2010.6.1.1.

[29] Bender B, Bornemann A, Reimold M, Ernemann U, Horger M. Imaging findings in autosomal-dominant arteriopathy with subcortical infarcts and leukoencephalopathy (CADASIL) - CADASIL - the most frequent familial stroke syndrome. Rofo 2012;184(8):679-683. http://dx.doi.org/10.1055/s-0032-1318829.

[30] Aracki-Trenkic A, Stojanov D. Imaging characteristics of CADASIL patient with inherited and de novo gene NOTCH 3Q19 mutation. [Accessed 10 October 2014] Retrieved from: http://posterng.netkey.at/esr/viewing/index.php?module=viewing_poster&doi=10.1594/ecr2014/C-0309. http://dx.doi.org/10.1594/ecr2014/C-0309

[31] Chabriat H, Levy C, Taillia H, Iba-Zizen MT, Vahedi K, Joutel A, et al. Patterns of MRI lesions in CADASIL. Neurology 1998;51(2):452-457. http://dx.doi.org/10.1212/WNL.51.2.452.

[32] Benisty S, Reyes S, Godin O, Hervé D, Zieren N, Jouvent E, et al. White-matter lesions without lacunar infarcts in CADASIL. Alzheimers Dis 2012;29(4):903-911. DOI:10.3233/JAD-2012-111784.

[33] Skehan SJ, Hutchinson M, MacErlaine DP. Cerebral autosomal dominant arteriopathy with subcortical infarcts and leucoencephalopathy: MR findings. AJNR Am J Neuroradiol 1995;16(10):2115-2119.

[34] Coulthard A, Blank S, Bushby K, Kalaria RN, Burn DJ. Distribution of cranial MRI abnormalities in patients with symptomatic and subclinical CADASIL. Br J Radiol 2000;73(867):256-265. http://dx.doi.org/10.1259/bjr.73.867.10817040.

[35] De Guio F, Mangin JF, Duering M, Ropele S, Chabriat H, Jouvent E. White Matter Edema at the Early Stage of Cerebral Autosomal-Dominant Arteriopathy With Subcortical Infarcts and Leukoencephalopathy. Stroke 2015;46(1):258-261. http://dx.doi.org/10.1161/STROKEAHA.114.007018.

[36] O'Sullivan M, Jarosz JM, Martin RJ, Deasy N, Powell JF, Markus HS. MRI hyperintensities in the temporal lobe and external capsule in patients with CADASIL. Neurology 2001;56(5):628-634. http://dx.doi.org/10.1212/WNL.56.5.628.

[37] Auer DP, Putz B, Gossl C, Elbel G, Gasser T, Dichgans M. Differential lesion patterns in CADASIL and sporadic subcortical arteriosclerotic encephalopathy: MR imaging study with statistical parametric group comparison. Radiology 2001;218(2):443-451. http://dx.doi.org/10.1148/radiology.218.2.r01fe24443.

[38] Marcus HS, Martin RJ, Simpson MA, Dong YB, Ali N, Crosby AH, et al. Diagnostic strategies in CADASIL. Neurology 2002;59(8):1134-1138. http://dx.doi.org/10.1212/WNL.59.8.1134.

[39] Kobayashi J, Sato S, Okumura K, Miyashita F, Ueda A, Ando Y, et al. Cerebral autosomal dominant arteriopathy with subcortical infarcts and leukoencephalopathy without anterior temporal pole involvement: a case report. Stroke Cerebrovasc Dis 2014;23(3):e241-242. http://dx.doi.org/10.1016/j.jstrokecerebrovasdis.2013.10.013.

[40] Hacinski V, Iadecola C, Petersen RC, Breteler MM, Nyenhuis DL, Black SE, et al. National Institute of Neurological Disorders and Stroke – Canadian Stroke Network vascular cognitive impairment harmonization standards. Stroke 2006;37(9):2220-2241. http://dx.doi.org/10.1161/01.STR.0000237236.88823.47.

[41] Mendes Coelho VC, Bertholdo D, Ono SE, de Carvalho Neto A. MRI hydrographic 3D sequences in CADASIL. Neurology 2014;82(4):371. http://dx.doi.org/10.1212/WNL.0000000000000056.

[42] Moody DM, Bell MA, Challa VR. The corpus callosum, a unique whitte-matter tract: anatomic features that may explain sparing in Binswanger disease and resistance to the flow of fluid masses. Am J Neuroradiol 1988;9(6):1051-1059.

[43] De Guio F, Reyes S, Duering M, Pirpamer L, Chabriat H, Jouvent E. Decreased T1 contrast between gray matter and normal-appearing white matter in CADASIL. AJNR Am J Neuroradiol 2014;35(1):72-76. http://dx.doi.org/10.3174/ajnr.A3639.

[44] Yao M, Hervé D, Jouvent E, Duering M, Reyes S, Godin O, et al. Dilated perivascular spaces in small-vessel disease: a study in CADASIL. Cerebrovasc Dis 2014;37(3):155-163. http://dx.doi.org/10.1159/000356982.

[45] Bokura H, Kobayashi S, Yamaguchi S. Distinguishing silent lacunar infarctions from enlarged Virchow-Robin spaces: a magnetic resonance imaging and pathological study. J Neurol 1998;245(2):116-122. http://dx.doi.org/10.1007/s004150050189.

[46] Koennecke HC. Cerebral microbleeds on MRI: prevalence, associations, and potential clinical implications. Neurology 2006;66(2):165-171. http://dx.doi.org/10.1212/01.wnl.0000194266.55694.1e.

[47] Vitali P, Boghen D, Daneault N, Guillon-Létourneau L, Poppe AY. Cerebral microbleed causing an acute stroke-like episode in a CADASIL patient. Can J Neurol Sci 2014;41(5):661-663. http://dx.doi.org/10.1017/cjn.2014.29.

[48] Oh SI, Kim SH, Kim HJ. Massive pontine microbleeds in a patient with CADASIL. JAMA Neurol 2014;71(8):1048-1049. http://dx.doi.org/10.1001/jamaneurol.2014.45.

[49] De Guio F, Reyes S, Vignaud A, Duering M, Ropele S, Duchesnay E, et al. In vivo high-resolution 7 Tesla MRI shows early and diffuse cortical alterations in CADASIL. PLoS One 2014;9(8):e106311. http://dx.doi.org/10.1371/journal.pone.0106311.

[50] Lian L, Li D, Xue Z, Liang Q, Xu F, Kang H, et al. Spontaneous intracerebral hemorrhage in CADASIL. J Headache Pain 2013;14:98. http://dx.doi.org/10.1186/1129-2377-14-98.

[51] Rinnoci V, Nannucci S, Valenti R, Donnini I, Bianchi S, Pescini F, et al. Cerebral hemorrhages in CADASIL: report of four cases and a brief review. J Neurol Sci 2013;330(1-2):45-51. http://dx.doi.org/10.1016/j.jns.2013.04.002.

[52] Schrag M, Greer DM. Clinical associations of cerebral microbleeds on magnetic resonance neuroimaging. J Stroke Cerebrovasc Dis 2014;23(10):2489-2497. http://dx.doi.org/10.1016/j.jstrokecerebrovasdis.2014.07.006.

[53] Gunda B, Porcher R, Duering M, Guichard JP, Mawet J, Jouvent E, et al. ADC histograms from routine DWI for longitudinal studies in cerebral small vessel disease: a field study in CADASIL. PLoS One 2014;9(5):e97173. http://dx.doi.org/10.1371/journal.pone.0097173.

[54] Holtmannspotter M, Peters N, Opherk C, Martin D, Herzog J, Brückmann H, et al. Diffusion magnetic resonance histograms as a surrogate marker and predictor of disease progression in CADASIL: a two-year follow-up study. Stroke 2005;36(12):2559-2565. http://dx.doi.org/10.1161/01.STR.0000189696.70989.a4.

[55] Liem MK, Lesnik Oberstein SA, Versluis MJ, Maat-Schieman ML, Haan J, Webb AG, et al. 7 T MRI reveals diffuse iron deposition in putamen and caudate nucleus in CADASIL. J Neurol Neurosurg Psychiatry 2012;83(12):1180-1185. http://dx.doi.org/10.1136/jnnp-2012-302545.

[56] Yamada K, Sakai K, Akazawa K, Sugimoto N, Nakagawa M, Mizuno T. Detection of early neuronal damage in CADASIL patients by q-space MR imaging. Neuroradiology 2013;55(3):283-290. http://dx.doi.org/10.1007/s00234-012-1105-x.